Fermi enhancement and band-gap renormalization of $Al_xGa_{1-x}As$/GaAs modulation-doped quantum wells

S. Haacke*
Institut für Festkörperphysik I, Technische Universität Berlin, Hardenbergstrasse 36, W-1000 Berlin 12, Federal Republic of Germany

R. Zimmermann
Max-Planck-Arbeitsgruppe im Institut für Grundlagen der Halbleikrphysik-Quantenstrutcturen, Hausvogteiplatz 5-7, O-1086 Berlin, Federal Republic of Germany

D. Bimberg
Institut für Festkörperphysik I, Technische Universität Berlin, Hardenbergstrasse 36, W-1000 Berlin 12, Federal Republic of Germany

H. Kal†
Max-Planck-Institut für Festkörperforschung, Heisenbergstrasse 1, W-7000 Stuttgart 80, Federal Republic of Germany

D. E. Mars and J. N. Miller
Hewlett Packard Laboratories, 3500 Deer Creek Road, Palo Alto, California 94304
(Received 10 December 1990; revised manuscript received 22 July 1991)

A comparative study of photoluminescence and photoluminescence-excitation spectra of thin n- and p-type modulation-doped $Al_xGa_{1-x}As$/GaAs quantum wells is presented for sheet carrier densities up to 10^{12} cm^{-2}. Photoluminescence-excitation spectra reveal a rather weak enhancement of the oscillator strength at the Fermi edge which is not observable in the emission spectra. The renormalization of the quasi-two-dimensional band gap is obtained by comparison with undoped quantum wells of the same width. The experimental data compare favorably with our calculations of the band-gap renormalization within the local-density approximation as well as with the self-energy shifts of electron and hole subbands calculated within the random-phase approximation. The importance of a detailed line-shape analysis for the separation of intrinsic and extrinsic components in the photoluminescence spectra is emphasized.

I. INTRODUCTION

High carrier density effects in quasi-2D (two-dimensional) semiconductor quantum-well (QW) structures are of considerable interest from a fundamental point of view in order to test many-particle theories of structures with reduced dimensionality.[1-5] Also such effects are important for the modeling of devices operating under high carrier injection conditions, such as semiconductor lasers.[6] Most publications deal with the shrinkage of the fundamental energy gap E_g, the so-called band-gap renormalization (BGR) which is due to exchange and correlation interactions. In a confined system the separation of charges, introduced by modulation doping, leads to a bending of the band profile. The resulting shift of the sublevels is included in the definition of BGR used in this paper.

At given well width the BGR increases monotonically with the two-dimensional carrier concentration N_s, following roughly an $N_s^{1/3}$ dependence at low temperatures.[1] At fixed N_s, the BGR is slightly larger for smaller well width.[7] If the BGR is expressed in QW-dependent excitonic units, the existence of an universal relation (independent of the semiconductor material) for BGR (N_s) was recently proposed to exist for quasi-2D structures.[3]

The dynamic response of an electron Fermi sea to the presence of optically generated holes gives rise to an enhanced interaction of correlated electron-hole pairs near the Fermi level, resulting in an enhanced oscillator strength for optical transitions at the Fermi edge,[8,9] referred to as Fermi enhancement or Fermi-edge singularity. Modulation-doped quantum wells (MDQW's) are unique systems for the optical investigation of both effects, since a confined dense Fermi sea, spatially separated from the dopant atoms, can be easily investigated under low excitation conditions. Until now, most optical studies of modulation-doped QW's dealt with well widths larger than 8 nm in which the carrier confinement has a minor effect on BGR.

For the Fermi enhancement, contradictory results on In-Ga-As and GaAs QW's have been published. A comparative study of In-Ga-As/Al-In-As n-type MDQW's using optical emission and absorption spectroscopy was presented by Cingolani, Stolz, and Ploog.[4] Their samples showed the Fermi-edge singularity in the absorption spectrum whereas in emission the weak hole population at $\mathbf{k}=\mathbf{k}_F$ made photoluminescence (PL) from the Fermi

edge undetectable.

On the other hand photoluminescence spectra of In-Ga-As/InP n-type MDQW's obtained by Skolnick *et al.*[10] were interpreted as showing a pronounced Fermi-edge singularity (see also Ref. 11). The authors argued that alloy fluctuations in the metal-organic chemical-vapor deposition grown In-Ga-As QW's will lead to a violation of $\mathbf{k}$ conservation, making a recombination of electrons at $\mathbf{k}=\mathbf{k}_F$ with holes at the top of the valence band ($\mathbf{k}=\mathbf{0}$) possible.

For n-type GaAs QW structures, several authors report observations of the Fermi-edge singularity in absorption or excitation spectroscopy,[12,13] whereas others[14,15] show PL spectra with a shoulder at the high-energy side interpreted as being caused by the Fermi-edge singularity.

In the present paper, we present results of comparative photoluminescence (PL) *and* excitation (PLE) spectroscopy investigations of thin (width <8 nm) n- and p-type MDQW's as well as of undoped reference samples. PL and PLE measurements at different sample temperatures provide exhaustive information about the impact of many-body effects on the optical properties. From a comparison of PL and PLE spectra on an n-type 7.5-nm MDQW it is seen that the weak Fermi-edge singularity visible in PLE is not detectable in PL because of $\mathbf{k}$ conservation. Furthermore, the band-gap shifts we obtain reveal an enhancement of the BGR with increasing carrier confinement, in agreement with recent investigations on two-component plasma.[16]

II. SAMPLES AND EXPERIMENTAL DETAILS

The samples are grown by molecular-beam epitaxy on semi-insulating (100) GaAs substrates on top of which GaAs and $Al_{0.42}Ga_{0.58}As$ buffer layers with widths of 500 and 300 nm, respectively, were deposited. Three single GaAs quantum wells (SQW's) of 1.6, 4.6, and 7.5 nm width are sandwiched between $Al_{0.42}Ga_{0.58}As$ barriers (32 or 44 nm thick). The layer sequence is capped by a 300-nm $Al_{0.42}Ga_{0.58}As$ layer. In the modulation-doped samples, 20 nm of each barrier are n-type (Si-) or p-type (Be-) doped, leaving an undoped 12-nm-spacer at both sides of each SQW. The nominal doping concentration is either 10^{16} or 10^{18} cm^{-3}. We will concentrate here on results of samples with doping concentrations of 10^{18} cm^{-3} with $1.5\times10^{11}\leq N_s\leq9.0\times10^{11}$ cm^{-2} for well width L_z ranging between 1.6 and 7.5 nm.

The fact that, for a given doping concentration, the sheet carrier density N_s decreases with L_z is a result of our self-consistent calculations that can be understood as follows. In the case of n-type doping, for instance, N_s is determined by the difference $\Delta=E_F-E_1$, between the electronic Fermi energy E_F and the $n=1$ electron subband E_1. E_F is pinned on the energetic position of the neutral shallow Si donors in the barriers and is hence independent of the well width. E_1, on the other hand, increases with decreasing well width. For smaller well width Δ decreases and so does the sheet carrier density N_s.

This argument is, however, not rigorously correct, since the band bending lowers Δ by pushing E_1 upwards on the energy scale. This effect leads to a lower value of Δ than for a flat-band case. The monotonic increase of N_s with increasing L_z is, however, still valid.

For the BGR determination the undoped sample serves as a reference. For this reason, the growth rate (1 μm/h) and the substrate temperature (620 °C) were exactly the same for the undoped and the modulation-doped samples in order to obtain identical QW widths. The growth was interrupted for 20 s at both sides of each QW leading to a smoothing of the GaAs/Al-Ga-As interface but also to an undesired impurity incorporation as can be seen from the unusually big difference between the peak positions of PL and PLE spectra of the undoped sample [10 meV in Fig. 3(b)].

The PL spectra that we discuss here are recorded in the temperature range of 1.8–300 K under low-excitation conditions (typically 5 W/cm^2), i.e., the optically generated carrier density was below 10^{10} cm^{-2}. An Ar^+ laser ($\lambda=514.5$ nm) was used for excitation. The spectral resolution of the 0.5-m monochromator was 1 Å or 0.2 meV.

Time integrated PLE spectra were obtained by exciting the samples with a dye laser (pulse length of 5 ps) synchronously pumped with a mode-locked argon ion laser at a repetition rate of 80 MHz. The luminescence is dispersed in a 2-m double monochromator at the end of which a GaAs photomultiplier and a subsequent photon-counting system are mounted. Low-excitation conditions were also applied. The detection energy was set to the peak positions of the PL spectra.

III. EXPERIMENTAL RESULTS

The temperature dependence of the PL of the undoped as well as of the modulation-doped samples reveals that the spectra consist of an unresolved doublet. As an example, the PL spectra of the n-type doped 4.6-nm SQW are plotted in Fig. 1. We observe a displacement of the PL maximum to higher energies when the temperature is

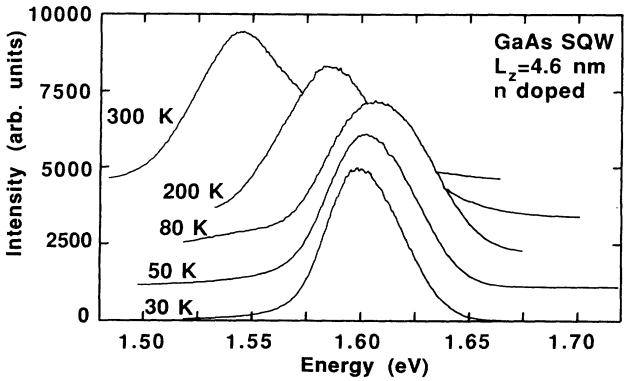

FIG. 1. Temperature dependence of the PL spectra for the n-type doped 4.6-nm SQW. Between 30 and 80 K a blueshift of the PL peak is observed indicating the competition between extrinsic and intrinsic emission.

raised from 30 to 80 K. For still higher temperatures the PL maximum follows the common GaAs $E_g(T)$ dependence.[17] This anomalous temperature behavior is explained by the fact that the intrinsic $(e,\mathrm{hh})_1$ transition gains in intensity with respect to an extrinsic band-to-impurity $[(e,A^0)]$ transition, which disappears due to thermal ionization.

For the undoped samples we observe a similar behavior (not shown here). Here, the unresolved doublet consists of the $n=1$ exciton and most presumably of the neutral acceptor bound exciton (A^0,X) transition.[18,19] The latter interpretation is confirmed by a relatively large difference of the peak position in the 6-K PL and PLE spectra (12 meV for $L_z=4.6$ nm) which cannot be explained by a simple Stokes shift, related to a thermalization induced by interface roughness.[20,21]

The distinction between the two PL components is crucial for the determination of both the renormalized and the unrenormalized band gap. This is achieved by a careful line-shape analysis taking an inhomogeneous broadening due to interface roughness into account. The method of line-shape analysis for undoped QW's is described in detail in Refs. 21 and 22. For the spectra of the MDQW's the following formula is used in order to derive the renormalized band gap E_g':[23]

$$I(E)\propto \mathrm{erfc}\left[\frac{E-E_g'}{\sqrt{2}\sigma}\right] \times \frac{\exp\left[-\frac{m_e}{M}(E-E_g')\Big/kT_c\right]}{\exp\left[\left[\frac{m_h}{M}(E-E_g')-E_F^e\right]\Big/kT_c\right]+1} \quad (1)$$

($M=m_e+m_h$).

Recombination of free electrons and holes under **k** conservation and in parabolic subbands is assumed. The thermalized hole population is expressed by the Boltzmann distribution function. The Fermi distribution with the electron Fermi energy E_F^e describes the one-component electron plasma. The Fermi energy is determined from the Burstein-Moss shift of the PLE spectra as described below. Well-width fluctuations due to interface roughness result in a broadening of the steplike 2D density of states which is expressed by the complementary error function $\mathrm{erfc}(x)$.[21] We therefore have three fit parameters E_g',σ and the carrier temperature T_c. The extrinsic components are simply accounted for by a Gaussian line shape with a broadening parameter σ_{ex} and centered at the transition energy $E(e,A^0)$ or $E(A^0,X)$ for the n-type doped or undoped sample, respectively.

Our line-shape analysis demonstrates the separation of the intrinsic and extrinsic component. Starting with the 300-K spectrum which is completely intrinsic we can follow the temperature dependence of the $(e,\mathrm{hh})_1$ transition down to 120 K by using the common $E_g(T)$ dependence. At lower temperatures an extrinsic component becomes important. This component may be isolated by extrapolating the $(e,\mathrm{hh})_1$-transition energy towards lower temperatures. Such a decomposition would not be possible with only one low-temperature spectrum. A typical example of line-shape analysis is shown in Fig. 2 (30-K PL spectrum of Fig. 1). We attribute the extrinsic component here to a (e,A^0) transition because of its large energy difference as compared to the intrinsic $(e,\mathrm{hh})_1$ transition of 29.2 meV.

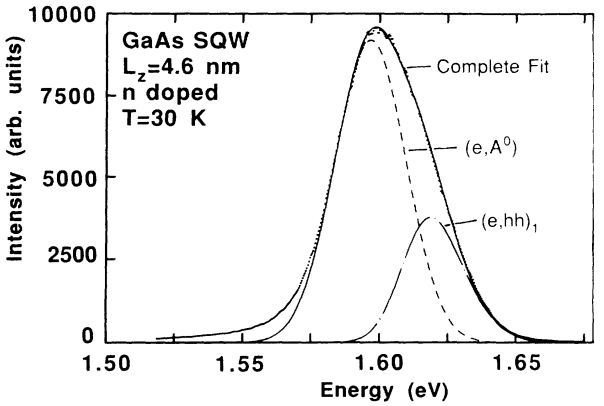

FIG. 2. The line shape of the 30-K spectrum of Fig. 1 is resolved by a detailed line-shape analysis. The two components are attributed to a (e,A^0) and a $(e,\mathrm{hh})_1$ transition at the renormalized band gap E_g'. The solid line presents a comparison of the sum of both components to the experimental spectrum (dotted).

Two remarks should be made in order to stress the importance of the line-shape analysis. The PL peak resulting from the addition of both PL components is 27 meV lower in energy than the $(e,\mathrm{hh})_1$ transition (1.626 eV), which is the relevant one for the BGR determination. Using the overall maximum would lead to an erroneous BGR result. Furthermore, the peak position of the intrinsic $(e,\mathrm{hh})_1$ component is displaced by 7 meV with respect to the actual transition energy, the difference being due to inhomogeneous broadening. The correct position of the renormalized $(e,\mathrm{hh})_1$ band gap can therefore only be obtained by such a detailed line-shape analysis. The presence of the extrinsic component still limits the accuracy of the approach, since the intensity ratio between the two components is difficult to determine. A typical uncertainty for the renormalized $(e,\mathrm{hh})_1$ band gap is ± 1.5 meV.

As an illustration of our approach to the determination of the BGR(N_s) data we discuss in detail the spectra of the 4.6-nm SQW in the n-type doped and the undoped sample. For the n-type doped 4.6-nm SQW we find the renormalized band gap to be $E_g'=1.6285$ eV (± 2 meV) at 2 K. The best PL fit was obtained with a carrier temperature $T_c=15$ K and a Gaussian broadening parameter $\sigma=11.5$ meV, the intrinsic component being displayed in Fig. 3(a) as a dashed line.

The sheet carrier density N_s of the MDQW's due to modulation doping is deduced from the Burstein-Moss shift E_F^c observed in the PLE spectra. For the n-type doped 4.6-nm SQW shown in Fig 3(a) the onset of the PLE spectra is shifted by E_F^c with respect to the renormalized gap E_g'. In a parabolic approximation and for n-

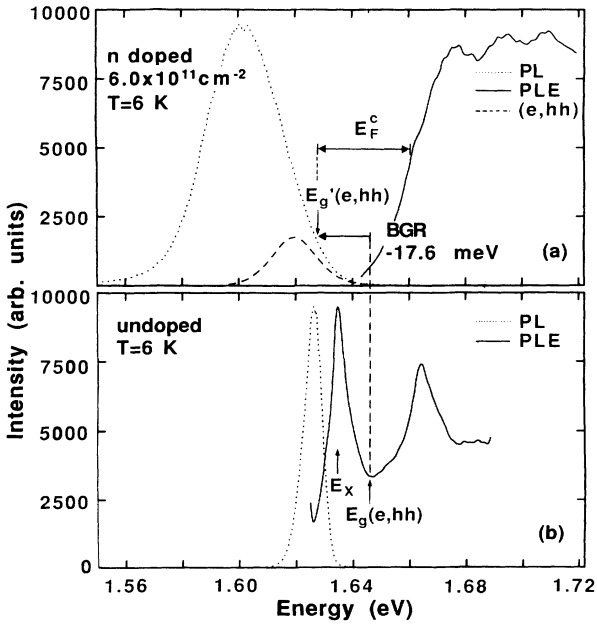

FIG. 3. PL (dotted lines) and PLE spectra (solid lines) of the (a) n-type doped and (b) undoped 4.6-nm SQW. The dashed line shape of (a) is the intrinsic band-to-band component of the PL spectrum. The band-gap renormalization BGR between E_g and E_g' is indicated as well as the Burstein-Moss shift E_F^c. E_x in (b) denotes the heavy-hole exciton line.

type doping, E_F^c is related to the electron Fermi energy E_F^e by

$$E_F^c = \left[1+\frac{m_e}{m_{\rm hh}}\right] E_F^e \ . \tag{2}$$

Here we use the effective electron mass $m_e=0.0665$ and, for the effective "in-plane" hole mass, a value of $m_{\rm hh}=0.112$.[17] For the n-type doped 4.6-nm SQW we find the Burstein-Moss shift $E_F^c=32.5\pm3.0$ meV and hence $N_s=6.0\times10^{11}$ cm^{-2} ($\pm9\%$). The accuracy of N_s is mainly limited by the uncertainty of E_g' discussed above. An independent N_s determination as recently proposed by Boettcher *et al.*[24] would be highly desirable.

The BGR value is obtained by comparison of E_g' with the unrenormalized band gap of the undoped 4.6-nm SQW. This procedure yields a value that can be directly compared to the theoretical results because our self-consistent band profile calculations account for both the exchange-correlation interactions and the band bending given by Poisson's equation. Due to the very small thickness of our SQW's it turns out, however, that band bending modifies the $(e,{\rm hh})_1$-transition energy only very little (<2 meV). The observed redshift of the PL lines can therefore be attributed to the exchange-correlation interactions alone.

The low-temperature PLE spectrum plotted in Fig. 3(b) (together with the PL spectrum) yields an excitonic transition energy E_x of 1.6530 eV (±1 meV). With an exciton binding energy of 11.1 meV,[25] we determine the unrenormalized gap to be at $E_g=1.6461$ eV (±1 meV). We

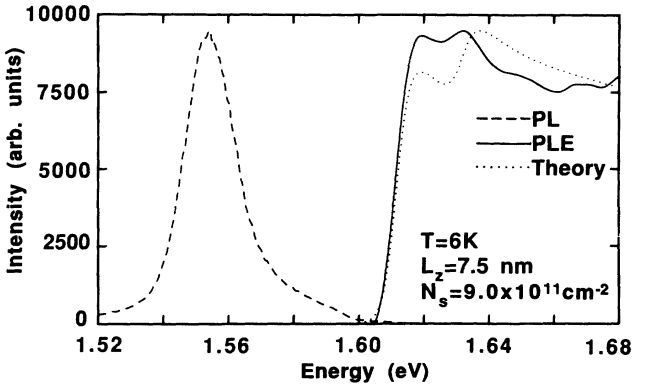

FIG. 4. PL (dashed line) and PLE (solid line) spectra of the n-type doped 7.5-nm SQW at 6 K. The Fermi resonances observed in the PLE spectrum are clearly absent in emission. The calculated absorption coefficient (dotted line) is plotted for comparison.

thus obtain a BGR value of -17.6 ± 3.0 meV for the n-type doped SQW. The same approach is carried out for the other n- or p-type doped SQW's. A summary of the results and a comparison with calculations is presented in the next paragraph.

The most important result, however, concerns the *Fermi enhancement.* Typical low-temperature PL and PLE spectra of a 7.5-nm SQW with a sheet carrier density of $N_s=9.0\times10^{11}$ cm^{-2} are depicted in Fig. 4. In the PLE spectrum we observe two small peaks at 1.618 and 1.632 eV with a larger intensity than the continuum observed for energies above 1.640 eV. According to Ref. 13 we attribute the two peaks to "Fermi-edge singularities" or Mahan excitons related to the $(e,{\rm hh})_1$ and $(e,{\rm lh})_1$ subband transitions with a wave vector $\mathbf{k}_\parallel\approx\mathbf{k}_F$, the Fermi wave vector.

The PL spectrum is, once again, a composition of intrinsic and extrinsic luminescence. The PL peak at 1.554 eV is a superposition of the (e,A^0) and the $(e,{\rm hh})_1$ transition at $\mathbf{k}_\parallel=0$. The PL shoulder near 1.59 eV is related to the $n=1$ light-hole subband. A comparison of its energetic position with calculations of the complex valence-band structure allows us to interpret this shoulder as a transition from the $n=1$ electron subband to the $n=1$ lh subband at a wave vector $|\mathbf{k}|\neq0$ ($<|\mathbf{k}_F|$) where the lh subband exhibits a horizontal tangent giving rise to a relatively large transition probability. It should be pointed out that we only see a very weak luminescence intensity in the region of the Fermi edge. In particular, the already rather weak Fermi enhancement found in the PLE spectrum is not visible in the emission spectrum. This result is in contrast with earlier publications,[10,11,15] where an enhanced emission in the high-energy tail was claimed to reveal a Fermi-edge singularity. In Refs. 10 and 11 hole localization (due to alloy fluctuations or electric field) is believed to relax $\mathbf{k}$ conservation and thus allows for such a pronounced luminescence.

For comparison we calculated the absorption coefficient for $\mathbf{k}$-conserving transitions between the $n=1$ heavy- as well as the $n=1$ light-hole subbands and the electronic Fermi sea. The screened ladder approximation

was used, with quasistatic screening in random-phase approximation (RPA). The inhomogeneous Schrödinger equation for an electron-hole pair was solved in **k** space by matrix inversion, following Wu.[26] In addition to Ref. 26, we have used the potential form factors in the Coulomb attraction as well as in the screening, and the self-consistently determined confinement wave function provided the input. Nondiagonal screening in the sublevel index was found to be negligible. The broadening of the sublevel states accounts for the inhomogeneous effect (quantum-well roughness) as well as for lifetime broadening. It acts to smooth the steplike onset of the absorption and reduces somewhat the Fermi enhancement. For the result plotted in Fig. 4 we used the Gaussian broadening parameter σ and the carrier temperature T_c that we found by fitting the PL spectra ($\sigma = 6.0$ meV; $T_c = 15$ K). Compared with the PLE spectrum the calculated $(e,\mathrm{lh})_1$ transition is rather strong. Two reasons may be responsible for the deviation. First, we assumed parabolic subbands for the calculation; the complex valence band would have led to **k**-dependent matrix elements. Second, PLE spectra might differ from absorption spectra, since absorption and relaxation processes are simultaneously observed by this technique. A comparison with the calculated absorption coefficient is therefore questionable. In addition, very recent theoretical work[5] reveals that the ladder approximation, which is used here, tends to overestimate the Fermi enhancement.

IV. BGR: COMPARISON WITH CALCULATIONS

For a given sheet density N_s the confinement wave functions and sublevels are calculated in the local-density approximation (LDA). Two different local exchange-correlation potentials (V_{xc}) account for the electron-electron and electron-hole interactions as proposed by Bauer and Ando.[27] For p-type doping, the V_{xc}'s are simply exchanged. An alternative and, from a theoretical point of view, more accurate way is to calculate the self-energy shifts of the $n=1$ electron and heavy-hole subband directly within the RPA using the actual confinement wave functions for the screened Coulomb potential. Details can be found in Ref. 6. A complete comparison of the calculations with the experimental data is depicted in Figs. 5(a) and 5(b).

In the case of n-type doping the 7.5-nm SQW has a BGR value slightly higher than the calculated ones. The deviation for the 4.6-nm SQW (4.5 meV) grown in a separate sample can be explained by a well width being one monolayer smaller than assumed, as it is also observed in PLE spectra of lower doped SQW's not shown here. All the BGR data discussed here therefore need to be carefully considered, since we assume identical QW widths for the undoped and the highly doped samples.

Nevertheless, the agreement between experiment and both theoretical approaches is quite satisfactory for the p-type doped 1.6- and 4.6-nm SQW's, even in the simple approximation of parabolic hole subbands. There are unfortunately no BGR data available for the p-type doped 7.5-nm SQW since the higher temperature spectra, indispensable for the analysis, interfere with the spectra of

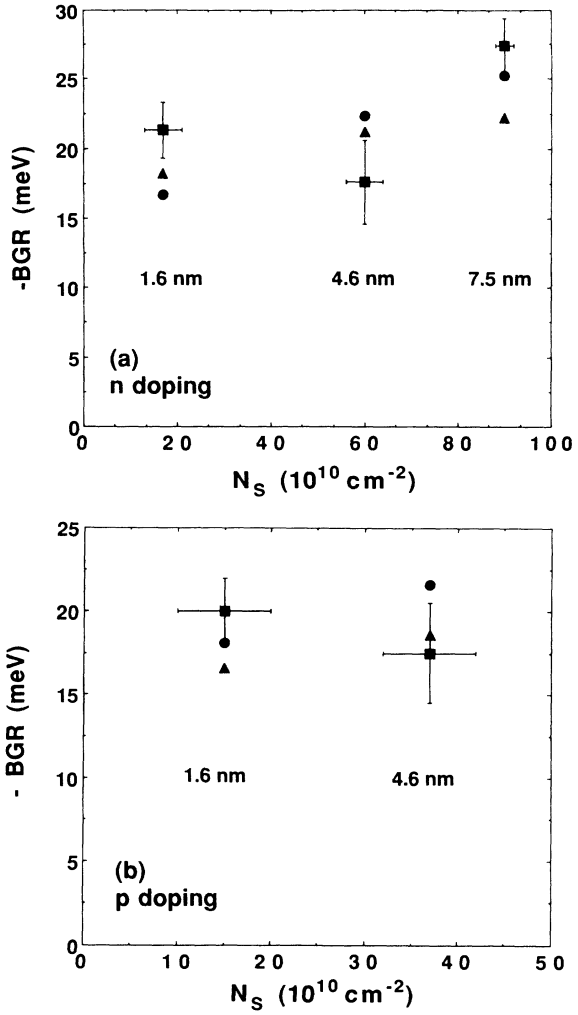

FIG. 5. Comparative representation of the BGR values for (a) n- and (b) p-type doping and for the well widths under study. The experimental data (squares) agree well with the calculations in the LDA (circles) and the complete self-energy approach (triangles).

the 4.6-nm SQW. It is worth noting that for both doping types the experimental BGR value of the thin 1.6-nm SQW's is higher than in the 4.6-nm SQW's although their sheet carrier density is much lower. The BGR value at fixed sheet density N_s depends on L_z also (see, for instance, Ref. 16), in analogy with the exciton binding energy which has it maximum at $L_z = 1.7$ nm.[25] Although our experiments are carried out for different N_s in the different wells, the general trend is in accordance with the well-width dependence of the BGR.

V. CONCLUSIONS

We have experimentally and theoretically determined the band-gap renormalization and Fermi enhancement in n- and p-type modulation-doped SQW's of 1.6, 4.6, and 7.5 nm width. The experimental data are derived from PL and PLE spectra. For both doping types the dependence of BGR on sheet density N_s and well width L_z is

investigated by direct comparison with undoped SQW's of the same width. Good agreement is obtained with realistic calculations in both the LDA and the full self-energy approach. BGR data of very thin wells ($L_z = 1.6$ nm) demonstrate an enhancement of BGR with respect to larger wells although the carrier density is lower.

A detailed analysis of the PL line shape is crucial for the separation of the intrinsic and extrinsic components present in our PL spectra. Doing so, there is nevertheless a limited accuracy for the determination of N_s and the renormalized band gap E_g' in any line-shape analysis. An independent determination of both quantities would be desirable.

A Fermi-edge singularity can be observed in the low-temperature PLE spectra of the n-type doped 7.5-nm SQW. In the PL spectra, however, this enhancement is not observed, in contrast to earlier reports.

ACKNOWLEDGMENTS

We are much indebted to Dr. R. K. Bauer for expert experimental help. The work at Technische Universität Berlin was funded by DFG in the framework of SFB 6.

*Present address: Service National des Champs Intenses, Centre National de la Recherche Scientifique, Boîte Postale 166X, F-38042 Grenoble CEDEX, France.

†Present address: Fachbereich Physik der Universitat Kaiserslantern, Erwin-Schrödinger-Strasse, Bau 46 W-6750 Kaiserslantern, Federal Republic of Germany.

[1]S. Schmitt-Rink, C. Ell, and H. Haug, Phys. Rev. B **33**, 1183 (1986).

[2]G. Tränkle, H. Leier, A. Forchel, H. Haug, E. Ell, and G. Weimann, Phys. Rev. Lett. **58**, 419 (1987).

[3]S. Das Sarma, R. Jalabert, and S.-R. Eric Yang, Phys. Rev. B **41**, 8288 (1990).

[4]R. Cingolani, W. Stolz, and K. Ploog, Phys. Rev. B **40**, 2950 (1989).

[5]T. Uenoyama and L. J. Sham, Phys. Rev. Lett. **65**, 1048 (1990).

[6]R. Zimmermann, E. H. Böttcher, N. Kirstaedter and D. Bimberg, Superlatt. Microstruct. **7**, 433 (1990).

[7]G. E. W. Bauer, Surf. Sci. **229**, 374 (1990).

[8]G. Mahan, *Many-Particle Physics*, 2nd ed. (Plenum, New York, 1990).

[9]A. E. Ruckenstein, S. Schmitt-Rink, and R. C. Miller, Phys. Rev. Lett. **26**, 504 (1986).

[10]M. S. Skolnick, J. M. Rorison, K. J. Nash, D. J. Mowbray, P. R. Tapster, S. J. Bass, and A. D. Pitt, Phys. Rev. Lett. **58**, 2130 (1987).

[11]Y. H. Zhang, D. S. Jiang, R. Cingolani, and K. Ploog, Appl. Phys. Lett. **56**, 2195 (1990).

[12]G. Livescu, D. A. B. Miller, and D. S. Chemla, Superlatt. Microstruct. **4**, 359 (1988).

[13]H. Kalt, K. Leo, R. Cingolani, and K. Ploog, Phys. Rev. B **40**, 12 017 (1989).

[14]J. S. Lee, Y. Iwasa, and N. Miura, Semicond. Sci. Technol. **2**, 675 (1987).

[15]S. Munnix, D. Bimberg, D. E. Mars, J. N. Miller, E. C. Larkins, and J. S. Harris, Superlatt. Microstruct. **6**, 369 (1989).

[16]V. D. Kulakovski, E. Lach, A. Forchel, and D. Gruetzmacher, Phys. Rev. B **40**, 8087 (1989).

[17]*Physics of Group IV Elements and III-V Compounds*, edited by O. Madelung, Landolt-Börnstein, New Series, Vol. 17a (Springer-Verlag, Berlin, 1982).

[18]R. Köhrbrück, S. Munnix, D. Bimberg, E. C. Larkins, and J. S. Harris, Appl. Phys. Lett. **54**, 623 (1989).

[19]S. Munnix, R. K. Bauer, D. Bimberg, J. S. Harris, R. Köhrbrück, E. C. Larkins, Ch. Maierhofer, D. E. Mars, and J. N. Miller, J. Vac. Sci. Technol. B **4**, 1014 (1989).

[20]C. Colvard, D. Bimberg, K. Alavi, Ch. Maierhofer, and N. Nouri, Phys. Rev. B **39**, 3419 (1989).

[21]J. Christen and D. Bimberg, Phys. Rev. B **42**, 7213 (1990).

[22]D. Bimberg, J. Christen, T. Fukunaga, H. Nakashima, D. E. Mars, and J. N. Miller, J. Vac. Sci. Technol. B **5**, 1191 (1987).

[23]A. Pinczuk, J. Shah, R. C. Miller, A. C. Gossard, and W. Wiegmann, Solid State Commun. **50**, 735 (1984).

[24]E. H. Boettcher, N. Kirstaedter, M. Grundmann, D. Bimberg, C. Harder, and H. P. Meier, in *Proceedings of the 20th International Conference on the Physics of Semiconductors*, edited by E. Anastassakis and J. D. Joannopolous (World Scientific, Singapore, 1990), p. 371.

[25]D. B. Tran Thoai, R. Zimmermann, M. Grundmann, and D. Bimberg, Phys. Rev. B **42**, 5906 (1990).

[26]J.-W. Wu, Phys. Rev. B **39**, 7992 (1989).

[27]G. E. W. Bauer and T. Ando, J. Phys. C **19**, 1537 (1986).